THE CRITICAL DIAMETERS FOR RAINFALL ATTENUATION IN SOUTHERN AFRICA

Oluwumi Adetan* and Thomas J. O. Afullo

School of Electrical, Electronic & Computer Engineering, University of KwaZulu-Natal, Durban 4041, South Africa

Abstract—This paper investigates the influence of critical raindrop diameters on the specific rain attenuation in Durban ($29°52'$S, $30°58'$E), South Africa. The total rainfall attenuation is evaluated by integrating over all the raindrop sizes and the differential change in the attenuation is observed over a given range of drop size diameters. The major contribution to the specific attenuation for the drop size distribution (DSD) models considered is created by the raindrop diameters not exceeding 2 mm especially at higher frequencies. The three parameter lognormal and gamma distribution models are employed for the purpose of analysis. For the DSD models considered in this work, the total percentage fraction created by raindrops in the diameter range $0.5 \text{ mm} \leq D \leq 2.5 \text{ mm}$ and $1 \text{ mm} \leq D \leq 3 \text{ mm}$ to the total specific attenuation is found to be critical for the overall and seasonal rainfall attenuation at 2.5 GHz–100 GHz in Durban. It is observed that the total specific attenuation increases with increased frequencies and a higher rainfall rate produces high rain attenuation. In this paper, both the overall and seasonal values of $R_{0.01}$ determined for Durban are used.

1. INTRODUCTION

Attenuation on radio propagation paths is generally caused by various atmospheric components such as gases, water vapour, clouds and rain. Rain attenuation, caused by scattering and absorption by the water droplets is one of the most important signal impairments influencing the attenuation of microwave (3–30 GHz) and millimetre wave (30–300 GHz) [1]. The nearly linear relationship existing between the rainfall rate R (mm/h) and the specific attenuation A_s at 35 GHz has

been known since 1940s and was successfully tested experimentally for estimating path-averaged rainfall rate in the early 1960s. This linearity was also found to be independent of the (rain) drop size distribution, DSD [2]. The study of drop size distribution (DSD) is however, vital for several application areas such as satellite meteorology, microwave communications, cloud physics and soil erosion [3]. The drop size distribution is an important parameter for the estimation of attenuation due to rain at microwave and millimeter-wave frequency applications because it governs all the microwave and rainfall integral relation.

It has been established that modeling of DSD in tropical and temperate regions is not the same. This is due to the presence of heavy rainfall in tropical regions compared to temperate regions. Measurements of drop size distributions in tropical regions are few when compared to temperate regions where a large database exists. The negative exponential function as proposed by Marshall and Palmer [4] or the Laws and Parsons Model [5] and the gamma distribution model often characterize modeling of raindrop size distributions in the temperate region. However, there is so much uncertainty in the preponderance and estimation of small diameter raindrops due to limitation in the sensitivity of the measuring equipment. These models grossly overestimate the concentration of the small diameter raindrops in the tropical regions hence the Ajayi and Olsen (1985) [6] model was proposed and found suitable for the modelling of tropical rain drop size distributions and equally adequate for the determination of the specific attenuation.

2. PREVIOUS WORK DONE ON RAINFALL RATE AND DSD MODELS IN DURBAN

Several works have been done by researchers on rainfall attenuation and raindrop size distribution in the tropical and equatorial regions, as well as in Durban (29°52′S, 30°58′E), South Africa [7–17]. In 2006, Owolawi [10] estimated the M-P parameters for Durban and defined the intercept parameter (drop density per unit volume), N_0. In his findings, he established a power law relation for the intercept given by $N_0 = a_1 R^{a_2}$ with a_1 and a_2 were estimated as 1500 and 0.26 respectively. In 2010, Odedina and Afullo [11] proposed the lognormal and the modified gamma distribution models as best fit for the measurements of rainfall in Durban. Afullo [12], while studying the rain drop size distribution model for the eastern coast of South Africa established that the optimised lognormal and gamma DSD models compete favourably well with the DSD obtained for same tropical

regions using the Biweight kernel estimation technique for Durban. While using the Maximum Likelihood Estimation (MLE) technique, Owolawi [13] proposed the lognormal model as the best fit for modeling DSD in Durban. In their study, Alonge and Afullo [14] considered the rainfall drop size distributions for different seasons-summer, autumn, winter and spring; they established that the lognormal model is suitable for summer and autumn; the modified gamma for winter and Weibull distribution is best for the spring season in Durban. The values of $R_{0.01}$ for the different season were also estimated. Recently, Adetan and Afullo [15, 16] in separate studies compared the two methods to evaluate the lognormal raindrop size distribution model in Durban and the three-parameter raindrop size distribution modeling for microwave propagation in South Africa. They established that the method of moment (MoM) provides a better technique to estimate the DSD parameters in Southern Africa with the lognormal model giving the best fit. In their findings, they showed that the three-parameter lognormal DSD gives a better fitting and performance when compared with the gamma distribution model. However, the gamma distribution model is also adequate as the error deviation is minimal. In 2011, Akuon and Afullo [17] derived the rain cell sizes for the southern Africa and estimated the overall $R_{0.01}$ for Durban as 60 mm/h. The seasonal and overall values of $R_{0.01}$ determined by [14] and [17] are used in this work for the evaluation of the drop size distribution, $N(D)$ parameters required for the estimation of the rainfall specific attenuation.

It is worth mentioning at this juncture that no work has been done to determine the influence of particular raindrop channels (or diameters) at which the rain attenuation is affected significantly in Durban and the Southern Africa region. This paper therefore, seeks to investigate these critical diameters that produce a major contribution to the total specific attenuation in Durban. The Mie scattering approximation at temperature of 20°C for spherical raindrop shape is adopted for the estimation of the scattering functions k and α. In this paper, the lognormal and gamma distribution models are used to characterize the measured rain drop size distribution $N(D)$ in Durban as determined in [15].

3. PREVIOUS INVESTIGATIONS ON CRITICAL DIAMETERS

Within the tropical region and other parts of the globe, a number of researchers have investigated the particular contribution of certain drop diameters to the rain attenuation. Lee et al. [19, 20] investigated the DSD for Singapore using the lognormal DSD model and identified

the critical range of diameters as 0.771 mm to 5.3 mm. They
established that while removing consecutive rain diameters (channels),
lower diameters raindrops ($<$ 0.771 mm) contribute insignificantly
to the overall specific rain attenuation for the selected rain rates.
Similarly, the influence of particular raindrop diameters on rain
attenuation was also carried out by Fiser [21] in the Czech Republic.
The critical range of diameter contributing to the specific rain
attenuation was found to be approximately 0.7–1.5 mm. The prevailing
contribution to the specific attenuation was formed by raindrops of
diameters not exceeding 2 mm. In Malaysia, Lam et al. [22] while
investigating the specific raindrop sizes producing major contribution
to the total specific attenuation with $R = 120.4$ mm/h, established
that small and medium-size drops contributed more to the rainfall
attenuation as frequency increases. The oblate spheroid raindrop shape
was however adopted. Marzuki et al. [23] observed in Equatorial
Indonesia that the increasing role of small and medium-sized drops
to rain attenuation is proportional to frequency of transmission. In
their observation, the drop size that produced the largest contribution
to the specific attenuation for rain rate of 10 mm/h did not exceed
3 mm.

In this paper, we investigate the critical raindrop diameters
influencing the specific rain attenuation in Durban, South Africa using
the spherical raindrop shape at temperature $T = 20°$C. Our method
is to compute the total rainfall attenuation by integrating over all the
raindrop sizes and determine the differential change in the attenuation
as observed over a fixed diameter interval, dD_j ($= 0.1$ mm). The
diameter ranges contributing 90%, 99%, 99.5%, 99.9%, 99.99% and
100% to the total specific attenuation are also discussed. This range of
diameters constitutes the surface area under the curve and along the
abscissa regions.

4. RAINDROP SIZE DISTRIBUTION MODELS AND EXTINCTION CROSS SECTIONS

This section considers the measurements of the raindrop size
distribution models employed in the computation of the specific
attenuation. There are several DSD models used for raindrop
distribution modelling across the temperate and tropical regions. In
this paper, the lognormal and gamma DSD models are employed for
the estimation of the rainfall attenuation.

4.1. DSD Measurements and Models

Generally, the measured rain drop size distribution $N(D_j)$ from the disdrometer data is the number of raindrops per cubic meter per millimetre diameter $(\text{mm}^{-3}\text{m}^{-1})$ as adopted by [24, 25] is given as (1):

$$N(D_j) = \frac{n_j}{v(D_j) \times T \times A \times dD_j} \ (\text{mm}^{-3}\text{m}^{-1}) \qquad (1)$$

where n_j is the number of drops measured in the drop size bin, $v(D_j)$ is the terminal velocity of Gun and Kinzer's [25] water drops in m/s, T is the one-minute sampling time in $60\,\text{s}$, A is the measurement area of the disdrometer given as $0.005\,\text{m}^2$ and dD_j is the representative change in diameters interval of the bin in mm. As earlier stated, this work considers the analysis of the data in $0.1\,\text{mm}$ diameter interval from consecutive channels (bins). The precipitation rate, R (mm/h) can be determined from the measured DSD data as (2) [24]:

$$\left. \begin{aligned} R &= \tfrac{1}{6 \cdot A \cdot T} \pi \sum_{j=1}^{20} n_j D_j^3 \\ &= 6.28318536 \times 10^{-3} \sum_{j=1}^{20} D_j^3 n_j \end{aligned} \right\} \left[\frac{\text{mm}}{\text{h}} \right] \qquad (2)$$

A well-known integral equation of the rain rate R as computed from the DSD model is given by [25] as (3):

$$\left. \begin{aligned} R &= 6\pi \times 10^{-4} \int_0^{\infty} D_j^3 \cdot V(D_j) \cdot N(D_j) dD_j \ [\text{mm/h}] \\ &= 1.88496 \times 10^{-3} \sum_{j=1}^{20} D_j^3 \cdot V(D_j) \cdot N(D_j) dD_j \end{aligned} \right\} \qquad (3)$$

Equation (3) must not be violated by any DSD. Disdrometer measurements of raindrop size distribution used for the estimation of the DSD parameters in this paper were obtained from the J-W RD-80 disdrometer readings mounted at the rooftop of the School of Electrical, Electronic and Computer Engineering, University of KwaZulu-Natal, South Africa. Sample data obtained from the disdrometer over a period of about 27 months were above 80,000 samples. It should be mentioned that rainfall samples with overall sum of drops less than 10 were removed (ignored) from the data samples to compensate for the dead- time errors. The instrument is located at an altitude of 139.7 meters above sea level. The location site is free of noise and shielded from abnormal winds.

4.1.1. The Lognormal Distribution Model

The lognormal distribution model as proposed by Ajayi-Olsen (A-O) [6] was primarily for the tropical rainfall. The tropical lognormal model was adopted because of the peculiarity of the South Africa rainfall with tropical region [26]. The model is expressed by [6, 27] in the form of (4) as:

$$N(D) = \frac{N_T}{\sqrt{2\pi} \times \sigma \times D} \exp\left[-0.5\left(\frac{\ln(D) - \mu}{\sigma}\right)\right] \ (\text{m}^{-3}\text{mm}^{-1}) \quad (4)$$

where μ is the mean of $\ln(D)$, σ is the standard deviation which determines the width of the distribution and N_T (concentration of rainfall drops) is a function of climates, geographical location of measurements and rainfall type. One unique feature of the lognormal distribution is that $N(D)$ approaches zero as the drop diameter tends to zero. This model was found adequate and suitable for the modeling of drop size distribution in the tropical regions characterized with heavy rain rates [6]. The three parameters in (4) above are related to the rainfall rate R by [6] in the form (5)–(7) as:

$$N_T = a_0 R^{b_0} \quad (5)$$
$$\mu = A_\mu + B_\mu \ln R \quad (6)$$
$$\sigma^2 = A_\sigma + B_\sigma \ln R \quad (7)$$

where a_0, b_0, A_μ, B_μ, A_σ and B_σ are coefficients of moment regression determined using the least squares method of regression technique. The estimated parameters are represented in the scatter plots in Figure 1 as functions of rainfall rates using the method of moment.

Recently, Adetan and Afullo [15] proposed the three-parameter lognormal DSD model using the method of moments in a representative form (4) as given by (8)–(10) as:

$$\mu = -0.3104 + 0.1331 \ln R \quad (8)$$
$$\sigma^2 = 0.0738 + 0.0099 \ln R \quad (9)$$
$$N_T = 268.07 R^{0.4068} \quad (10)$$

4.1.2. The Gamma Distribution Model

The three-parameter gamma distribution model in Durban as expressed by Tokay and Short [18] in the form of (11) was similarly studied in [15] with N_o ($\text{m}^{-3}\text{mm}^{-1-\mu}$) indicating the scaling parameter, μ (unitless) is the shape parameter, and Λ is the slope parameter in mm^{-1}. While the shape parameter does influence the slope of the distribution at larger diameter bound, it contributes largely
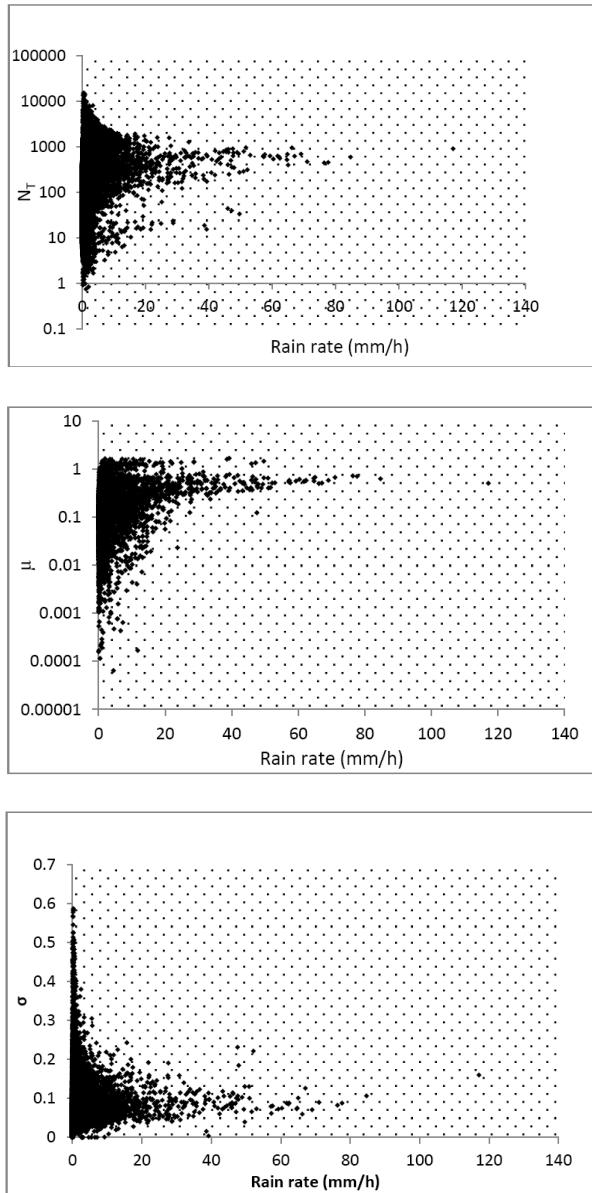
Figure 1. Scatter plot of the lognormal DSD parameters; N_T, μ and σ against rainfall rate R for the disdrometer data in Durban, South Africa.

Table 1. DSD parameters from disdrometer measurements in Durban.

Gamma DSD Model		
$\mu = 2$	$N_o = 78259R^{-0.156}$	$\Lambda = 6.3209R^{-0.168}$
Lognormal DSD Model		
$N_T = 268.07R^{0.4068}$	$\mu = -0.3104 + 0.1331 \ln R$	$\sigma = 0.0738 + 0.0099 \ln R$

on the curvature of the distribution at small diameters. The gamma distribution is particularly useful in tropical climate regions where the exponential distribution was found to be inadequate [6, 18].

$$N(D) = N_0 D_i^{\mu} \exp(-\Lambda D_i) \ [\text{m}^{-3}\text{mm}^{-1}] \tag{11}$$

with

$$\left.\begin{array}{c} \mu = 2 \\ N_0 = 78259R^{-0.156} \\ \Lambda = 6.3209R^{-0.168} \end{array}\right\} \tag{12}$$

The parameters in (8)–(10) and (12) above are used in this paper for the computation of the drop size distribution model, $N(D)$. The representative of the parameters discussed in Section 4.1 is shown in Table 1.

5. EVALUATION OF THE SPECIFIC RAINFALL ATTENUATION AND THE EXTINCTION CROSS SECTIONS

The specific attenuation A_s (dB/km) of microwave due to rain can be computed using (13):

$$A_s = 4.343 \times 10^{-3} \int\limits_{0}^{D_{\max}} Q_{ext}(D, \lambda, m) \cdot N(D)dD \ \left[\frac{\text{dB}}{\text{km}}\right] \tag{13}$$

where Q_{ext} is the extinction cross sections which is dependent on the drop diameter D, the wavelength λ, and the complex refractive index of water drop m, which in turn is a function of the frequency and temperature. The extinction cross section Q_{ext} is found by applying the classical scattering theory of Mie for a plane wave impinging upon a spherical absorbing particle. The Mie scattering theory is applied under the assumption that each spherical raindrop illuminated by a plane wave is uniformly distributed in a rain filled medium. Similarly, it is assumed that the distance between each drop is large enough to avoid any interaction between them. For more accurate modeling, the

raindrops should be modelled as oblate spheroids. The cross section Q_{ext} can be expressed by [28, 29] as (14):

$$Q(D, \lambda, m) = \frac{\lambda^2}{2\pi} \sum_{n=1}^{\infty} (2n + 1)\text{Re}[a_n + b_n] \tag{14}$$

where a_n and b_n are the Mie scattering coefficients.

The expression of the extinction cross sections, Q_{ext} provided by [11] as a frequency-dependent, power law function with coefficients, k and α is expressed in (15) and adopted in this paper; where k and α are the coefficients that depend on rain rate, temperature, polarization and canting angle.

$$Q_{ext}(D) = k \left(\frac{D}{2} \right)^{\alpha} \tag{15}$$

The Mätzler's MATLAB [30] functions are used for the estimation of k and α. Table 2 shows the computed values of k and α of the power law relation in (15) at frequencies of 2.5 to 100 GHz. The total rainfall attenuation therefore is evaluated by integrating over all the raindrop sizes. Substituting (4) and (15) in (13) for the lognormal DSD model, the total specific rain attenuation is computed numerically over the raindrop diameters as (16):

$$A_s = 4.343 \times 10^{-3} \int_{d_1}^{d_{\max}} k \left(\frac{D_j}{2} \right)^{\alpha}$$
$$\times \frac{N_T}{\sqrt{2\pi} \times \sigma \times D_j} \exp \left[-0.5 \left(\frac{\ln(D_j) - \mu}{\sigma} \right)^2 \right] dD_j \tag{16}$$

Table 2. k and α values at $f = 2.5$–100 GHz at $T = 20°$C.

Frequencies (GHz)	k	α
2.5	0.0048	3.3911
10	0.3857	4.5272
19.5	1.6169	4.2104
25	2.4567	4.0186
40	4.3106	3.5077
60	6.0493	3.0094
80	7.0623	2.6621
100	7.6874	2.4156

Equation (16) is solvedfrom the incremental values of the specific rain attenuation of (17):

$$dA_s = 4.343 \times 10^{-3} \frac{kN_T}{2^\alpha \sigma \sqrt{2\pi}} \left[D_j^{\alpha-1} \cdot e^{-t} \right] \cdot dD_j \qquad (17)$$

where

$$t = \frac{1}{2} \frac{((\ln D_j) - \mu)^2}{\sigma} \qquad (18)$$

Similarly, the total rain attenuation using the extinction cross sections (15) and integrating over the drop diameters gives the specific
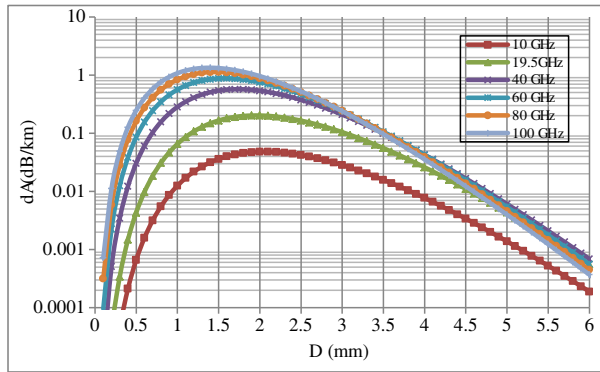
(a)

(b)

Figure 2. Overall specific attenuation against the drop size diameters at various frequencies. (a) Lognormal DSD model. (b) Gamma DSD model. $R_{0.01} = 60 \, \text{mm/h}$ [17].

attenuation for the gamma DSD model in (11), as (19):
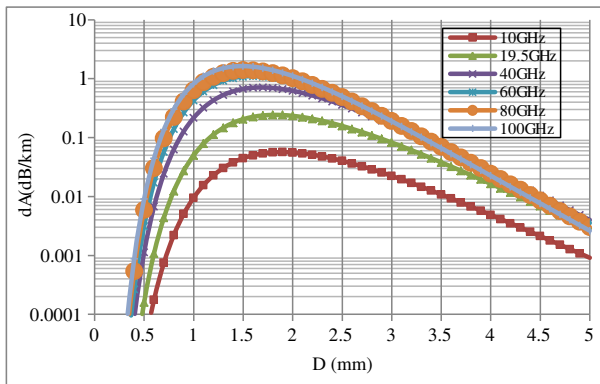
$$A_s = 4.343 \times 10^{-3} \int_{d_1}^{d_{\max}} k \left(\frac{D_j}{2} \right)^{\alpha} \times N_0 D_j^{\mu} \exp(-\Lambda j) dD_j \qquad (19)$$

Solving (19) gives (20):

$$dA_s = 4.343 \times 10^{-3} \frac{kN_0}{2^{\alpha}} \left[D_j^{\alpha+2} \cdot e^{-\Lambda D_j} \right] dD_j; \ (\mu = 2) \qquad (20)$$

6. OVERALL DETERMINATION OF CRITICAL DIAMETERS IN DURBAN

The critical diameters are the range of diameters over which the contribution to the rainfall attenuation is predominant. Figures 2(a) and (b) show the overall critical diameters versus the specific rainfall attenuation for the lognormal and gamma DSD models using the overall $R_{0.01}$ of 60 mm/h as determined by [17]. In Figure 2(a), it can be observed that the greatest shift of the attenuation towards drops of lower diameter occurs at the diameter $D \sim 1.4$ mm at 10 GHz; while at 100 GHz, it was observed to occur at $D \sim 1.1$ mm. For the gamma model in Figure 2(b), the maximum shift occurs around $D \sim 1.3$ mm at 10 GHz and diameter $D \sim 0.9$ mm at 100 GHz. This compares well with the results of [21]. The specific attenuation therefore is directly proportional to the surface area under the curve and above the diameters (x-axis). Tables 3(a) and (b) show the total

Table 3. Total rainfall specific attenuation created by drops in the diameter range $0.1 \geq D \geq 7$ mm at $f = 10$–100 GHz. (a) Overall ($R_{0.01}$ [17]). (b) Seasonal ($R_{0.01}$ [14]) for the lognormal (L-M) and gamma (G-M) DSD models in Durban.

	L-M	G-M
f (GHz)	A_s (dB/km)	A_s (dB/km)
10	0.961007	0.985026
19.5	3.977033	4.027874
40	10.73367	10.72919
60	15.72329	15.80689
80	19.23337	19.6010
100	21.82271	22.58165

(a)
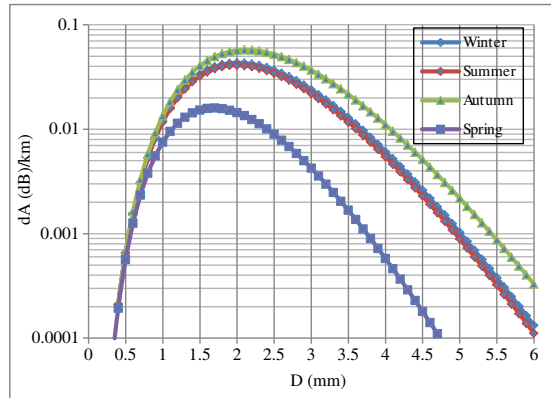
(a)
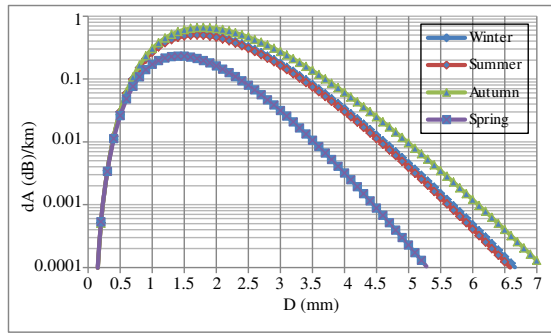
(b)

(c)

Figure 3. Seasonal specific attenuation against the drop size diameters (mm) at (a) $f = 10\,\text{GHz}$, (b) $f = 40\,\text{GHz}$, (c) $f = 100\,\text{GHz}$ for the gamma DSD model.
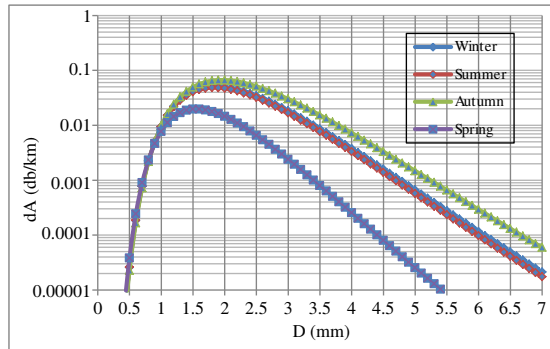
(a)
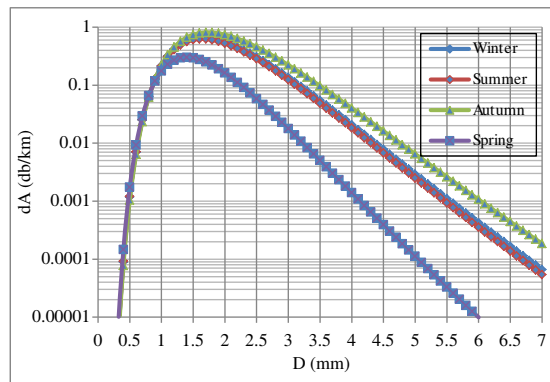
(b)
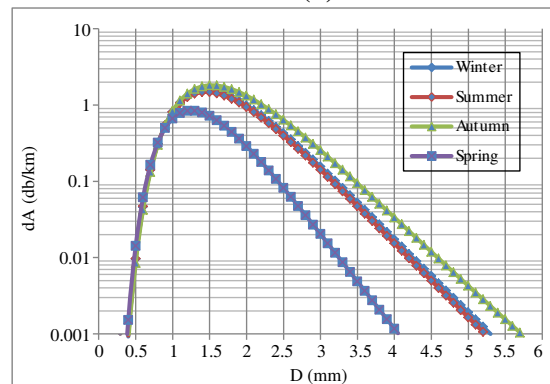
(c)

Figure 4. Seasonal specific attenuation against the drop size diameters at (a) $f = 10\,\mathrm{GHz}$, (b) $f = 40\,\mathrm{GHz}$, (c) $f = 100\,\mathrm{GHz}$ for the lognormal DSD model.

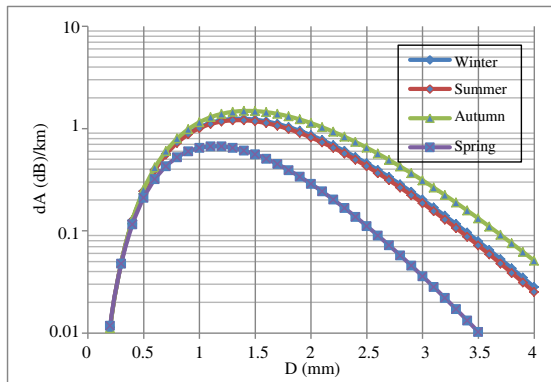| Season		L-M	G-M
	f (GHz)	A_s (dB/km)	A_s (dB/km)
Winter $(R_{0.01} = 50.48 \, \text{mm/h})$	10	0.843837	0.865123
	19.5	3.514999	3.559706
	40	9.621152	9.614014
	60	14.23015	14.30342
	80	17.52132	17.85711
	100	19.97118	20.67386
Summer $(R_{0.01} = 53.37 \, \text{mm/h})$	10	0.793249	0.813361
	19.5	3.314549	3.356609
	40	9.133414	9.125235
	60	13.57084	13.63964
	80	16.76166	17.08379
	100	19.14682	19.82421
Autumn $(R_{0.01} = 72.15 \, \text{mm/h})$	10	1.179336	1.208381
	19.5	4.830721	4.893022
	40	12.75207	12.75333
	60	18.39855	14.30342
	80	22.27487	22.69526
	100	25.09265	25.94920
Spring $(R_{0.01} = 18.51 \, \text{mm/h})$	10	0.260292	0.267478
	19.5	1.150270	1.164359
	40	3.356328	3.563353
	60	5.771739	5.792821
	80	7.540564	7.692947
	100	8.957303	9.305668

(b)

attenuation created by drops size in the diameter interval of 0.1 to 7 mm for the two models. The total specific rainfall attenuation increases with increasing frequency. At frequency above 40 GHz, it can be observed as illustrated in Tables 4 and 5 for the overall and seasonal determination of the critical diameters thatthe drop size diameters creating the prevailing contribution to the total attenuation for all the rain rates considered did not exceed 3 mm (90%). This confirms the result of [23]. Similarly, the role of small drops diameters increases with the increasing frequency for the DSD models as the prevailing

contribution of raindrops diameters to the specific attenuation does not exceed 2 mm, especially at higher frequencies. This is observed in Table 6 for the DSD models.

Table 4. Percentage fraction (%) of the overall specific attenuation created by particular diameter intervals to the total specific attenuation at $f = 10\text{--}100\,\text{GHz}$ for $R_{0.01} = 60\,\text{mm/h}$ [17].

f (GHz)	G-M Diameter Range (mm)	ΣA_s (dB/km)	L-M Diameter Range (mm)	ΣA_s (dB/km)	%
	0.7–3.5	0.8885	1.0–3.3	0.8681	90
	0.8–5.3	0.9759	0.6–4.6	0.9514	99
10	0.7–5.4	0.9797	0.9–5.6	0.9562	99.5
	0.6–6.3	0.9837	0.5–5.9	0.9600	99.9
	0.3–6.8	0.9849	0.4–6.7	0.9609	99.99
	0.2–6.9	0.9850	0.3–6.9	0.9601	100
	0.6–3.1	9.6613	0.8–2.9	9.6996	90
	0.7–5.7	10.616	0.4–4.0	10.605	99
40	0.6–5.8	10.678	0.6–4.5	10.683	99.5
	0.4–5.6	10.718	0.5–5.3	10.723	99.9
	0.3–6.7	10.728	0.5–6.4	10.732	99.99
	0.2–6.7	10.729	0.3–6.8	10.733	100
	0.5–2.8	17.744	0.6–2.6	17.329	90
	0.5–4.2	19.380	0.6–3.7	19.029	99
80	0.5–5.9	19.485	0.7–4.3	19.140	99.5
	0.3–5.3	19.585	0.4–4.7	19.208	99.9
	0.2–6.5	19.599	0.5–6.6	19.232	99.99
	0.2–6.9	19.600	0.3–6.7	19.233	100
	0.5–2.7	20.387	0.5–2.5	19.551	90
	0.4–4.0	22.374	0.6–3.6	21.590	99
100	0.3–4.2	22.475	0.4–3.9	21.706	99.5
	0.3–5.4	22.564	0.4–4.7	21.801	99.9
	0.2–5.9	22.579	0.5–6.1	21.820	99.99
	0.1–6.9	22.581	0.4–6.7	21.822	100

7. SEASONAL DETERMINATION OF CRITICAL DIAMETERS IN DURBAN

The values of $R_{0.01}$ for summer (50.48 mm/h), winter (53.37 mm/h), autumn (72.15 mm/h) and spring (18.51 mm/h) seasons as determined

Table 5. Percentage fraction (%) of the seasonal specific attenuation created by particular diameter intervals to the total specific attenuation at (a) $f = 10$ GHz, (b) $f = 100$ GHz for $R_{0.01}$ [14].

Season	G-M Diameter Range (mm)	ΣA_s (dB/km)	L-M Diameter Range (mm)	ΣA_s (dB/km)	%
Winter $(R_{0.01} = 50.48$ mm/h)	0.8–3.5	0.7858	0.6–3.2	0.7665	90
	0.4–4.8	0.8533	0.3–4.5	0.8356	99
	0.6–5.1	0.8606	0.9–5.5	0.8392	99.5
	0.5–6.1	0.8645	0.7–6.1	0.8432	99.9
	0.4–6.7	0.8650	0.3–6.6	0.8437	99.99
	0.3–6.8	0.8651	0.2–6.9	0.8438	100
Summer $(R_{0.01} = 53.37$ mm/h)	0.4–3.4	0.7359	0.6–3.2	0.7245	90
	0.8–5.7	0.8070	0.7–4.5	0.7861	99
	0.7–5.6	0.8099	0.9–5.6	0.7890	99.5
	0.7–5.9	0.8126	0.5–5.5	0.7921	99.9
	0.4–6.7	0.8132	0.3–6.6	0.7931	99.99
	0.3–6.9	0.8133	0.3–6.9	0.7932	100
Autumn $(R_{0.01} = 72.15$ mm/h)	0.5–3.6	1.0908	1.0–3.4	1.0634	90
	0.4–4.8	1.1932	1.0–5.2	1.1703	99
	0.6–5.4	1.2027	0.8–5.3	1.1735	99.5
	0.5–6.1	1.2071	0.6–6.3	1.1786	99.9
	0.3–6.7	1.2082	0.6–6.8	1.1791	99.99
	0.2–6.8	1.2084	0.2–6.9	1.1793	100
Spring $(R_{0.01} = 18.51$ mm/h)	0.7–2.9	0.2416	0.8–2.6	0.2359	90
	0.4–3.8	0.2639	0.3–3.7	0.2582	99
	0.6–4.8	0.2663	0.7–4.0	0.2590	99.5
	0.5–5.7	0.2672	0.7–5.3	0.2599	99.9
	0.3–6.1	0.2674	0.5–5.6	0.2602	99.99
	0.2–6.8	0.2675	0.2–6.9	0.2603	100

(a) 10 GHz

Season	G-M Diameter Range (mm)	ΣA_s (dB/km)	Diameter Range (mm)	L-M ΣA_s (dB/km)	% Contribution
Winter ($R_{0.01} = 50.48$ mm/h)	0.4–2.6	18.613	0.6–2.5	18.095	90
	0.5–4.0	20.374	0.3–3.6	19.801	99
	0.4–4.6	20.584	0.4–3.8	19.861	99.5
	0.3–5.9	20.660	0.6–5.5	19.958	99.9
	0.2–6.1	20.672	0.4–6.1	19.969	99.99
	0.2–6.8	20.673	0.3–6.7	19.97	100
Summer ($R_{0.01} = 53.37$ mm/h)	0.6–2.7	17.874	0.6–2.5	17.439	90
	0.5–4.6	19.613	0.4–3.5	18.959	99
	0.4–4.5	19.732	0.6–3.9	19.059	99.5
	0.3–6.4	19.811	0.6–4.9	19.127	99.9
	0.2–6.2	19.823	0.5–6.3	19.145	99.99
	0.2–6.8	19.824	0.3–6.5	19.147	100
Autumn ($R_{0.01} = 72.15$ mm/h)	0.5–2.8	23.507	0.3–2.6	22.562	90
	0.4–4.0	25.668	0.2–3.7	24.820	99
	0.4–4.6	25.828	0.5–4.1	24.972	99.5
	0.3–5.7	25.932	0.4–4.7	25.057	99.9
	0.2–6.2	25.947	0.5–6.2	25.090	99.99
	0.2–6.8	25.948	0.2–6.7	25.092	100
Spring ($R_{0.01} = 18.51$ mm/h)	0.6–2.4	8.384	0.7–2.1	8.119	90
	0.4–4.0	9.237	0.6–3.1	8.895	99
	0.3–3.5	9.260	0.4–3.1	8.910	99.5
	0.5–5.6	9.293	0.5–3.8	8.943	99.9
	0.2–6.9	9.304	0.4–4.8	8.956	99.99
	1.0–6.9	9.306	0.2–6.6	8.957	100

(b) 100 GHz

by [14] for Durban are used to estimate the seasonal critical range of diameters in this work. Figures 3 and 4 show the specific attenuation and the range of raindrop diameters at $f = 10$ GHz, 40 GHz and 100 GHz for the gamma and lognormal DSD models respectively. It can be observed that higher rainfall rates cause higher rainfall specific attenuation and the specific attenuation increases with increasing frequency for all seasons. Similarly as observed in Section 6, the largest

Table 6. Contributions (dB/km) of raindrop diameters to specific attenuation at $f = 10$–100 GHz. (a) Gamma. (b) Lognormal DSD models ($R_{0.01} = 60$ mm/h [17]).

Diameter (mm)	10 GHz	19.5 GHz	40 GHz	60 GHz	80 GHz	100 GHz
0.5	0.000664581	0.004322293	0.030523641	0.085469317	0.1614904	0.247393232
1	0.012517079	0.065358612	0.283590164	0.562162419	0.834930961	1.078171325
1.5	0.036054359	0.16556628	0.540282505	0.875074998	1.128957357	1.319192745
2	0.04814263	0.201819597	0.538044131	0.755066663	0.881508157	0.95953242
2.5	0.042184486	0.164772675	0.375526933	0.471539663	0.509451002	0.524864766
3	0.028317604	0.104400918	0.209324254	0.240016267	0.243402605	0.239746372
3.5	0.015816249	0.055531905	0.099911229	0.106090339	0.101978768	0.09670172
4	0.007721478	0.02598769	0.042568511	0.042291453	0.038810205	0.035610277
4.5	0.00340138	0.011028519	0.016630033	0.015580019	0.013724484	0.012232532
5	0.001381641	0.004332728	0.006067134	0.005393336	0.0045803	0.003977728
5.5	0.000525588	0.001599184	0.002094276	0.001775341	0.001458622	0.001237316
6	0.000189396	0.000560599	0.000690612	0.000560598	0.000446878	0.000371032
6.5	6.52142E-05	0.000188196	0.000219162	0.000170947	0.000132533	0.000107889
7	2.16018E-05	6.08923E-05	6.73133E-05	5.0601E-05	3.82336E-05	3.05609E-05

(a) 10 GHz

Diameter (mm)	10 GHz	19.5 GHz	40 GHz	60 GHz	80 GHz	100 GHz
0.5	2.44494E-05	0.00015901	0.00112294	0.003144345	0.005941097	0.009101391
1	0.009552573	0.04987928	0.21642554	0.4290216	0.63718848	0.822820544
1.5	0.044693481	0.20523825	0.66974166	1.084755054	1.399471134	1.635289547
2	0.055845165	0.23410953	0.62412799	0.875872843	1.022544224	1.113051905
2.5	0.040321344	0.15749524	0.35894122	0.450713399	0.486950326	0.501683318
3	0.022364563	0.08245333	0.16531926	0.189559075	0.192233523	0.189345918
3.5	0.010830001	0.03802486	0.06841311	0.072644183	0.06982883	0.06621543
4	0.004884991	0.0164411	0.02693095	0.026755673	0.024553263	0.02252883
4.5	0.002126469	0.00689479	0.01039674	0.009740292	0.008580251	0.007647515
5	0.000911798	0.00285933	0.00400393	0.003559268	0.003022715	0.002625054
5.5	0.000389847	0.00118617	0.0015534	0.001316832	0.00108191	0.000917759
6	0.000167452	0.00049565	0.00061059	0.000495645	0.0003951	0.000328043
6.5	7.2591E-05	0.00020948	0.00024395	0.000190284	0.000147525	0.000120094
7	3.18489E-05	8.9777E-05	9.9244E-05	7.46042E-05	5.63702E-05	4.50578E-05

(b) Lognormal DSD model

contributions to the specific attenuation for DSD models considered are due to raindrop diameters not greater than 2 mm, for all seasons. Table 7 shows the contribution of the drop sizes in the range 0.1 mm $\leq D \leq 2.0$ mm, 0.5 mm $\leq D \leq 2.5$ mm, 1.0 mm $\leq D \leq 3.0$ mm, 1.5 mm $\leq$

Table 7. Percentage (%) fraction of the attenuation created by range ofraindrop diameters (mm) to the total attenuation within the given diameter range for (a) $R_{0.01} = 60\,\text{mm/h}$ [17] and (b) different seasons, $R_{0.01}$ [14].

	L-M	G-M	L-M	G-M	L-M	G-M	L-M	G-M	L-M	G-M
f (GHz)	$0.1{\leq}D{\leq}2$	$0.1{\leq}D{\leq}2$	$0.5{\leq}D{\leq}2.5$	$0.5{\leq}D{\leq}2.5$	$1{\leq}D{\leq}3$	$1{\leq}D{\leq}3$	$1.5{\leq}D{\leq}3.5$	$1.5{\leq}D{\leq}3.5$	$4{\leq}D{\leq}7$	$4{\leq}D{\leq}7$
10	45.97	39.58	70.71	62.75	85.02	78.04	80.64	77.32	3.28	4.94
19.5	50.24	44.32	74.28	67.06	86.99	80.29	74.46	76.12	2.57	3.93
40	59.63	55.31	81.31	75.94	90.13	83.33	75.19	71.03	1.45	2.25
60	65.99	63.16	85.50	81.37	91.30	83.50	70.92	65.42	0.93	1.44
80	70.19	68.46	88.00	84.59	91.60	82.49	67.42	60.63	0.68	1.04
100	73.02	72.08	89.59	86.54	91.54	81.15	64.71	56.85	0.53	0.81

(a)

Season		L-M	G-M	L-M	G-M	L-M	G-M	L-M	G-M	L-M	G-M
	f (GHz)	$0.1{\leq}D{\leq}2$	$0.1{\leq}D{\leq}2$	$0.5{\leq}D{\leq}2.5$	$0.5{\leq}D{\leq}2.5$	$1.0{\leq}D{\leq}3.0$	$1.0{\leq}D{\leq}3.0$	$1.5{\leq}D{\leq}3.5$	$1.5{\leq}D{\leq}3.5$	$4.0{\leq}D{\leq}7.0$	$4.0{\leq}D{\leq}7.0$
Winter	10	48.42	41.58	72.89	64.82	86.35	79.43	80.23	77.32	2.79	4.32
	19.5	52.67	46.35	76.30	69.02	88.11	81.45	78.79	75.84	2.18	3.42
	40	61.92	57.29	82.96	77.57	90.79	83.94	74.00	70.17	1.21	1.93
	60	68.13	65.01	86.87	82.72	91.65	83.69	69.43	64.24	0.77	1.23
	80	72.18	70.18	89.19	85.73	91.74	82.39	65.76	59.28	0.56	0.88
	100	74.89	73.69	90.65	87.53	91.55	80.86	62.96	55.41	0.44	0.68
Summer	10	49.59	42.54	73.91	65.79	86.94	80.06	79.98	77.27	2.58	4.04
	19.5	53.83	47.32	77.24	69.94	88.61	81.97	78.42	75.66	2.01	3.19
	40	63.01	58.23	83.71	78.32	91.07	84.19	73.39	69.73	1.11	1.79
	60	69.13	65.88	87.49	83.34	91.79	83.75	68.68	63.65	0.71	1.14
	80	73.11	70.99	89.73	86.25	91.78	82.31	64.94	58.61	0.51	0.81
	100	75.77	74.45	91.13	87.97	91.52	80.69	62.10	54.71	0.39	0.63
Autumn	10	42.21	36.52	67.16	59.45	82.71	75.67	80.94	77.05	4.17	6.05
	19.5	46.47	41.20	70.96	63.92	85.02	78.27	80.19	76.31	3.29	4.86
	40	56.01	52.20	78.57	73.27	88.88	82.17	76.79	72.15	1.89	2.83
	60	62.59	60.21	83.18	79.13	90.55	83.00	73.02	67.09	1.23	1.84
	80	66.98	65.69	85.99	82.67	91.17	82.45	69.81	62.61	0.90	1.33
	100	69.97	69.47	87.77	84.87	91.35	81.43	67.28	59.00	0.72	1.04
Spring	10	70.77	60.57	89.02	81.47	93.16	87.54	69.18	71.45	0.47	1.02
	19.5	74.16	65.01	90.81	84.27	93.12	87.38	65.86	67.82	0.35	0.77
	40	80.89	74.32	93.99	89.36	92.01	84.89	57.75	58.23	0.17	0.39
	60	84.93	80.20	95.67	91.89	90.36	81.16	51.61	50.44	0.10	0.23
	80	87.39	83.86	96.59	93.06	88.78	77.52	47.25	44.74	0.07	0.15
	100	88.95	86.21	97.14	93.55	87.44	74.44	44.16	40.63	0.05	0.12

(b)

$D \leq 3.5\,\text{mm}$ and $4.0\,\text{mm} \leq D \leq 7.0\,\text{mm}$ for the overall and seasonal determination of critical diameters. Over 80% of the attenuation at all frequencies for the models is contributed by drop diameters in the range $1.0\,\text{mm} \leq D \leq 3.0\,\text{mm}$ for the overall and seasonal values of $R_{0.01}$. The summer and winter seasons tend to have similar critical diameters at the same frequency range as shown in Table 7. At frequency of $80\,\text{GHz}$ and above, the critical range of diameters for the gamma DSD model occurs in the range $0.5\,\text{mm} \leq D \leq 2.5\,\text{mm}$. The highest contribution to the attenuation in the diameter range $4.0\,\text{mm} \leq D \leq 7.0$ is observed during the autumn season to be 6.05% (Table 7(b)). This is very low and insignificant. Therefore, larger diameters contribute little to the specific attenuation.

8. CONCLUSION

This paper considered the critical range of diameters at which the specific rainfall attenuation is most influenced. Our approach was to evaluate the total rain specific attenuation by integrating over all the raindrop sizes (diameters). The maximum (peak) value of the rain attenuation as found from the DSD models considered showed that the critical range of diameter occurs at the drops diameter in the range $0.5\,\mathrm{mm} \leq D \leq 2.5\,\mathrm{mm}$ and $1.0\,\mathrm{mm} \leq D \leq 3.0\,\mathrm{mm}$ for both the seasonal and overall values of $R_{0.01}$ in Durban. Over 80% of the attenuation at frequencies of 2.5–100 GHz for both the DSD models is created by drop diameters in the range $1.0\,\mathrm{mm} \leq D \leq 3.0\,\mathrm{mm}$ for the overall and seasonal values of $R_{0.01}$. The summer and winter seasons tend to have similar critical diameters at the same frequency range as shown in Table 7. For instance, at a frequency of 80 GHz and above, the critical range of diameters for the gamma DSD model occurs in the range $0.5\,\mathrm{mm} \leq D \leq 2.5\,\mathrm{mm}$. We conclude therefore that these ranges of diameter are critical to the overall determination of rain attenuation in Durban, South Africa. However, at larger diameters in the range $4.0\,\mathrm{mm} \leq D \leq 7.0\,\mathrm{mm}$, the highest percentage contribution to rainfall attenuation was observably small (6.05%). The highest contribution of raindrops diameters to the specific rain attenuation was created by drop diameters not exceeding $2\,\mathrm{mm}$, especially at higher frequencies. This confirms the results of [19–23]. The percentage contribution as created by given range of diameters at various frequencies and seasons to the total specific attenuation was also investigated. We conclude that at a frequency above 40 GHz, the drop size diameter that gives the largest contribution to the total attenuation for all the rain rates considered does not exceed $3\,\mathrm{mm}$ (90%). This is similar to the results obtained by [23]. A good understanding of this rainfall attenuation characteristic will be helpful to properly design adequate fade margin levels, achieve the expected quality of service in a radio communication system operating in the South Africa region and for the purpose of link budget design by the engineers and service providers in this particular area.

9. FUTURE WORK

Due to some assumptions made in the estimation of the specific attenuation may not be the same as the measured raindrop shape, our next future work will be to compare the results reported in this work with experimental attenuation measurements performed in the same region or attenuation data from satellite communications links.

ACKNOWLEDGMENT

REFERENCES

1. Mathews, P. A., *Radio Wave Propagation VHF and Above*, Chapman and Hall Ltd., 1965.

2. Kültegin, A. and S. E. A. Daisley, "Relationships between rainfall rate and 35-GHz rainfall attenuation and differential attenuation: Modelling the effects of raindrop size distribution, canting, and oscillation," *IEEE Transactions on Geoscience and Remote Sensing*, Vol. 40, No. 11, Nov. 2011.

3. Harikumar, R., S. Sampath, and V. S. Kumar, "An empirical model for the variation of raindrop size distribution with rain rate at a few locations in Southern India," *Advances in Space Research,* Vol. 43, 837–844, 2009.

4. Marshall, J. S. and W. M. Palmer, "The distribution of raindrops with size," *J. Meteor.*, Vol. 5, 165–166, 1948.

5. Laws, J. O. and D. A. Parsons, "The relation of raindrops size to intensity," *Trans. Am. Geophys. Union,* Vol. 24, 452–460, 1943.

6. Ajayi, G. O. and R. L. Olsen, "Modeling of a tropical raindrop size distribution for microwave and millimetre wave applications," *Radio Sci.*, Vol. 20, No. 2, 193–202, 1985.

7. Waldvogel, A., "The N_o jump of raindrop spectra," *J. Atmos. Sci.*, Vol. 31, 1067–1078, 1974.

8. Joss, J. and E. G. Gori, "Shapes of raindrop size distributions," *J. Appl. Meteorol*, Vol. 17, 1054–1061, 1978.

9. Ritcher, C., "On the parameterisation of drop size distributions-case studies with distrometer," *Internal Report of the Rutherford Appleton Laboratory*, UK, Dec. 14, 1995.

10. Owolawi, P. A., "Rain rate and raindrop size distribution models for line-of-sight millimetric system in South Africa," M.Sc. Thesis, University of KwaZulu Natal, Durban, 2006.

11. Odedina, M. O. and T. J. Afullo, "Determination of rain attenuation from electromagnetic scattering by spherical raindrops: Theory and experiment," *Radio Sci.*, Vol. 45, 2010.

12. Afullo, T. J. O., "Raindrop size distribution modeling for radio

link along the Eastern coast of South Africa," *Progress In Electromagnetics Research B*, Vol. 34, 345–366, 2011.

13. Owolawi, P., "Raindrop size distribution model for the prediction of rain attenuation in Durban," *PIERS Online*, Vol. 7, No. 6, 516–523, 2011.

14. Alonge, A. and T. J. O. Afullo, "Seasonal analysis and prediction of rainfall effects in Eastern South Africa at microwave frequencies," *Progress In Electromagnetics Research B*, Vol. 40, 279–303, 2012.

15. Adetan, O. and T. J. Afullo, "Three-parameter raindrop size distribution modeling for microwave propagation in South Africa," *Proceedings of The International Association of Science and Technology for Development (IASTED), International Conference on Modelling and Simulation (Africa MS 2012)*, 155–160, Gaborone, Botswana, Sep. 3–5, 2012, DOI:10-2316/P.2012.761-027.

16. Adetan, O. and T. J. Afullo, "Comparison of two methods to evaluate the lognormal raindrop size distribution model in Durban," *The SouthernAfrica Telecommunication Networks and Applications Conference (SATNAC)*, Fancourt, Western Cape, South Africa, Sep. 2–5, 2012.

17. Akuon, P. O. and T. J. O. Afullo, "Rain cell sizing for the design of high capacity radio link system in South Africa," *Progress In Electromagnetics Research B*, Vol. 35, 263–285, 2011.

18. Tokay, A. and D. A. Short, "Evidence from tropical raindrop spectra of the origin of rain from stratiform to convective clouds," *J. of Applied Meteorology*, Vol. 35, No. 3, 355–371, 1996.

19. Lakshmi, S. Y., H. Lee, and J. T. Ong, "The roles of particular raindrop size on rain attenuation at 11 GHz," *IEEE Xplore*, 1-4244-0983-7/07, ICICS, 2007.

20. Lee, Y. H., S. Lakshmi, and J. T. Ong, "Rain drop size distribution modelling in Singapore-critical diameters," *The Second European Conference on Antennas and Propagation (EUCAP)*, Nov. 11–16, 2007.

21. Fiser, O., "The role of particular rain drop size classes on specific rain attenuation at various frequencies with Czech data example," *Proceedings of ERAD*, 113–117, 2002.

22. Lam, H. Y., J. Din, L. Luini, A. D. Panagopoulos, and C. Capsoni, "Analysis of raindrop size distribution characteristics in Malaysia for rain attenuation prediction," *IEEE Xplore General Assembly and Scientific Symposium, XXXth URSI*, Aug. 13–20, 2011.

23. Marzuki, M., T. Kozu, T. Shimomai, W. L. Randeu, H. Hashiguchi, and Y. Shibagaski, "Diurnal variation of rain attenuation obtained from measurement of raindrop size distribution in Equatorial Indonesia," *IEEE Transactions on Antennas and Propagation*, Vol. 57, No. 4, 1191–1196, Apr. 2009.

24. Bartholomew, M. J., "Disdrometer and tipping bucket rain gauge handbook," DOE/SC-ARM/TR-079, ARM Climate Research Facility, Dec. 2009.

25. Gunn, R. and G. D. Kinzer, "Terminal velocity of fall for water drops in stagnant air," *J. Appl. Meteorology*, Vol. 6, 243–248, 1949.

26. Fashuyi, M. O., P. A. Owolawi, and T. J. Afullo, "Rainfall rate modelling for LOS radio systems in South Africa," *Africa Research J., South Africa Institute of Electrical Engineering*, Vol. 97, No. 1, 74–81, ISSN No. 1991–1696, Mar. 2006.

27. Adimula, I. A. and G. O. Ajayi, "Variations in raindrop size distribution and specific attenuation due to rain in Nigeria," *Annals of Telecommunications*, Vol. 51, Nos. 1–2, 1996.

28. Van de Hulst, H. C., *Light Scattering by Small Particles*, John Wiley and Sons Inc., New York, 1957.

29. Bohren, C. F. and D. R. Huffman, *Absorption and Scattering of Light by Small Particles*, John Wiley, Wienheim, 2004.

30. Mätzler, C., "Drop-size distributions and Mie computation," IAP Research Report 2002-16, University of Bern, Bern, Nov. 2002.